

## Structural, electronic and thermoelectric properties of LiAlX<sub>2</sub> (X=S and Se) chalcopyrites: promising for thermoelectric power generators

J. Kumari<sup>a</sup>, C. Singh<sup>b</sup>, R. Agrawal<sup>c</sup>, B. L. Choudhary<sup>a</sup>, A. S. Verma<sup>d,e,\*</sup>

<sup>a</sup>Department of Physics, Banasthali Vidyapith, Rajasthan, India, 304022

<sup>b</sup>Department of Physics, Agra College, Agra, India, 282002

<sup>c</sup>Department of Computer Engineering and Applications, G. L. A. University, Mathura, India, 281406

<sup>d</sup>Division of Research & Innovation, School of Applied and Life Sciences, Uttarakhand University, Uttarakhand, Dehradun – 248007, India

<sup>e</sup>University Centre for Research & Development, Department of Physics, Chandigarh University, Mohali, Punjab – 140413, India

Herein, we have inquired the structural, electronic and thermoelectric properties of the couple of chalcopyrite structured solids LiAlX<sub>2</sub> (X=S and Se) with the help of density functional theory (DFT), which is tracked by resolution of the Boltzmann transport equation with the constant relaxation time calculations. The LDA (Localized Density Approximation), PBE (Perdew-Burke-Ernzerhof), PBEsol (PBE functional revised for solids) and WC (Wu-Cohen) exchange correlation potentials have been used. The calculated lattice constants  $a = 5.271 \text{ \AA}$ ;  $c = 10.178 \text{ \AA}$  and  $a = 6.226 \text{ \AA}$ ;  $c = 12.165 \text{ \AA}$  for LiAlS<sub>2</sub> and LiAlSe<sub>2</sub> respectively and the band gap of the mentioned compounds are found in range from 1.74 eV to 3.13 eV. The dependency of thermoelectric parameters are calculated with different temperature (300-800K) and carrier concentration  $10^{18} \text{ } 10^{19} \text{ cm}^{-3}$ . From the study of ZT (figure of merit's  $ZT = S^2\sigma T/\kappa$  the dimensionless parameter) and it is found that it's value for both the compounds in n-type as well as in p-type region is 'unity'. Since these compounds can be the promising candidate for thermoelectric devices also these compounds are non-toxic, eco-friendly and good alternative for the green and renewable source of electric power generators.

(Received October 8, 2022; Accepted January 8, 2023)

*Keywords:* Chalcopyrites, Band gap, Seebeck coefficient, Figure of merit

### 1. Introduction

Now days, the humankind are facing a challenge that is how to fruitage energy in the form of electricity without disturbing environment. We are focused on chalcopyrite materials due to their wide applications in Lasers, LEDs, Photovoltaic cells, non-linear optical devices, non-toxicity etc. [1-6]. By making the combinations of the first, third and the sixth group elements, we got the direct band gap semiconductor material which is the fruitful output in photovoltaics. These chalcopyrite materials having wide range of absorption coefficient as well as extensive energy conversion efficiency [7-10] and also good for thin film solar cells [11]. As compare to other semiconducting compounds chalcopyrites are lower in toxicity which is suitable condition for environment. The currently reported studies reflects that these chalcopyrite semiconductors possess low resistivity and thermal conductivity due to which these compounds prove as potential candidate for thermoelectric generators (TEGs) [12,13]. We can obtain the enhanced sustainability of energy by ingesting of relapsed heat with the help of using thermoelectric generators (TEGs). A huge expanse of heat produces from trains, engines, homes and industrial areas which can be converted into electrical energy by using thermoelectric materials. Current studies on chalcogenide compounds ensure that these compounds are potential candidates as thermoelectric compounds [13]. A. Nomura *et al.* [14] and S. Twaha *et al.* [15] have been

---

\* Corresponding author: [ajay\\_phy@rediffmail.com](mailto:ajay_phy@rediffmail.com)  
<https://doi.org/10.15251/CL.2023.201.73>

presented that the tetragonal chalcopyrite structured solid as a substantial thermoelectric compound and their study confirms that this compound is good for TE-power generators. The instrument used for the above-mentioned conversion is called the thermoelectric power generators. As compare to other conversion devices the TEG having the fabulous benefits and they provide the sources having the long-life time, they are having eco-friendly nature. T. Ghellab *et al.* [16] have been investigated the structural, elastic, electronic as well as thermoelectric properties of  $XPN_2$  chalcopyrite structured solid, where  $X = Li, Na$  by using the first-principles study their study of thermoelectric properties likewise seebeck coefficient, electrical conductivity, thermal conductivity as well as figure of merit i.e., (ZT) found high value of ZT for the chosen compounds which is agreed to unity for n-types and p-types. Their study confirms that the chosen compounds are potential candidate for thermoelectric power generators (TEPGs). W. Khan *et al.* [17] have been investigated the thermoelectric properties of the polar chalcopyrite  $Li_2PbGeS_4$  the single crystal as the potential candidate for the photovoltaic applications by using the ab-initio calculations. Their study of thermoelectric parameter the outcomes of power factor confirms that the chosen compound is potential thermoelectric compound. V. V. Atuchin *et al.* [18] have been investigated  $LiGaTe_2$  tetragonal chalcopyrite solid's negative thermal expansion and the variation in the electronic structure for this solid. Their study found that the chosen compound is potential candidate for the linear as well as nonlinear optical properties in IR region and various applied applications. A. Kurus *et al.* [19] have been investigated the thermophysical properties of  $LiGaS_2$  chalcopyrite solid. Their observations ensure this compound is highly optical stable compound and this is the potential solid for manufacturing the various efficient thermoelectric devices. W. Sukkabot *et al.* [2] have been investigated the electronic structure and optical parameters of  $CuInTe_2$  chalcopyrite solid by using density functional theory. Their study confirms that this compound is good alternative for the solar cell applications. This research paper has been inspired by the various newly investigations on tetragonal chalcopyrite structured solids mainly lithium-based chalcopyrite solids. The framework of this research paper is as follows:

In section second, a short explanation of the theoretical background which is important to execute the calculations has been given. In section third, the results and opinions of the entire computation have been described. To the end, section four contains the conclusions of this research work.

## 2. Computational theory

For inquiring the structural, electronic and thermoelectric properties of  $LiAlX_2$  ( $X=S$  and  $Se$ ) chalcopyrite semiconductor materials we have performed the density functional theory (DFT) computation which is implemented in wien2k simulation package [20]. For these calculations we have used all electron full potential linearized augmented plane wave (FP-LAPW) [21] approach which is based on DFT. The K-S equation [22] has been resolved for a unit cell in LAPW method, by taking into consideration there are two pairs for two different domains i.e., one of it not overlap the atomic spheres which are situated on the atomic spots and another domain is the interstitial domain. In the inner side of muffin-tin sphere spherical harmonic expansion have been applied and at outer side of muffin-tin sphere plane wave basis set have been choose. In the spherical harmonics inside atomic spheres the density of charge and potential are extended here we have taken  $l_{max} = 10$ . The cut-off energy has been taken  $-6$  Ry. The  $R_{MT} * k_{max}$  has been taken 8, ( $R_{MT}$  stands for the minimum muffin tin radii of the atoms in the material's unit cell and the  $k_{max}$  stands for the maximum modulus of the reciprocal vector). The scf cycle converged at 0.00001 Ry (this is the energy difference in between the iterations) and the charge difference has taken been 0.0001e (e is the charge of electron). By minimizing the forces i.e., 1 mRy/Bohr which is acting upon the atoms we have been optimized the couple of crystal structure of ternary chalcopyrite semiconductors  $LiAlX_2$  ( $X=S$  and  $Se$ ). We have taken the  $G_{max}$ 's value 12 ( $G_{max}$  is the degree of the major vector in Fourier expansion of density of charge). The  $R_{MT}$  values for Li, Al, S ad Se-atoms are tabulated in the Table 1. The optimization of the structure, calculation of lattice parameters and the Scf calculation of the chosen compounds have been done by using the LDA [22], PBE, PBEsol, WC potentials [23-25]. We have found that the PBE-GGA potential gives us

the best result about lattice parameters, also by applying all the four mentioned exchange correlation potentials we have calculated the bandgaps of the chosen compounds and we found that PBE-GGA potential confirms the accuracy of band gaps. For calculating the structural and the electronic properties we have been taken  $7*7*7$  k-mesh in their first Brillouin zone. For calculating thermoelectric parameters, we have taken dense k-mesh  $40 * 40 * 40$  k-points by using the Boltz Trap code [26] at different temperature (300-800K) and electron and hole concentration from  $10^{18}$  -  $10^{19}$   $\text{cm}^{-3}$ .

Table 1. Values of  $R_{MT}$  (Muffin tin radii) of  $\text{LiAlX}_2$  ( $X=\text{S}$  and  $\text{Se}$ ).

$R_{MT}[\text{a.u}]$	Compounds	
	$\text{LiAlS}_2$	$\text{LiAlSe}_2$
Li	1.860	2.030
Al	2.060	2.270
X	1.960	2.500

### 3. Results and discussion

#### 3.1. Structural properties

The ternary chalcopyrite semiconductors generally grow in the tetragonal structure and from our study it is also confirm that the chosen ternary chalcopyrite compounds  $\text{LiAlX}_2$  ( $X=\text{S}$  and  $\text{Se}$ ) crystallizes into the body centred tetragonal which belongs to  $I42d$  space group it is derived from  $D_{2d}^{12}$  space group and the space group number is 122. Figure 1 shows the geometry of unit cells of  $\text{LiAlS}_2$  and  $\text{LiAlSe}_2$  compounds. The optimized lattice parameter curve as a function of total energy shown in Figure 2. In the geometry of crystal structure the atomic positions are as follows: the lithium (Li) atom located at  $(0, 0, 0);(0, 1/2, 1/4)$ , aluminium (Al) atom located at  $(1/2, 1/2, 0);(1/2, 0, 1/4)$  and sulphur/selenium (S/Se) atoms located at  $(u, 1/4, 1/8);(-u, 3/4, 1/8);(3/4, u, 7/8);(1/4, -u, 7/8)$  respectively. The optimized lattice constants  $a$  and  $c$  compared with experimentally calculated and calculated  $c/a$  ratio, the calculated bulk modulus ( $B$ ), the pressure derivative of bulk modulus ( $B'$ ), volume at equilibrium ( $V_0$ ) and total energy ( $E_0$ ) have been tabulated in Table 2. The optimization process has done by using the Murnaghan equation of state [27] employed into the simulation code. From the study of lattice parameters, it is concluded that our calculated lattice parameters agreed with experimental and other studies too. Also, this study of structural parameters ensures that the ternary chalcopyrite semiconductors are most stable in the body centred tetragonal symmetry.

Table 2. Calculated structural parameters compared with experimentally calculated values of  $\text{LiAlX}_2$  ( $X=\text{S}$  and  $\text{Se}$ ) ternary chalcopyrites.

Compounds	Lattice Constants [ $\text{\AA}$ ]		Lattice Constants [ $\text{\AA}$ ]		$c/a$	$B[\text{Gpa}]$	$B'$	$V_0$	$E_0[\text{Ry}]$
	$a$	$c$	$a$	$c$					
$\text{LiAlS}_2$	5.271	10.178	5.386 <sup>(a)</sup>	10.67 <sup>(a)</sup>	1.931	72.090	4.218	986.190	-4182.109
$\text{LiAlSe}_2$	6.226	12.165	6.351 <sup>(a)</sup>	12.01 <sup>(a)</sup>	1.953	54.763	4.458	1156.794	-20414.640

<sup>(a)</sup> Ref [28].

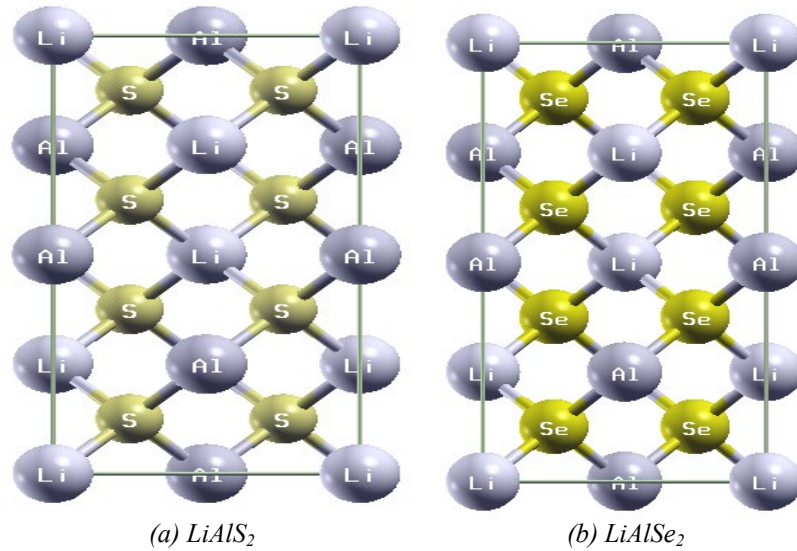


Fig. 1. Shows the crystal structure of  $\text{LiAlX}_2$  ( $X=\text{S}$  and  $\text{Se}$ ) ternary chalcopyrites

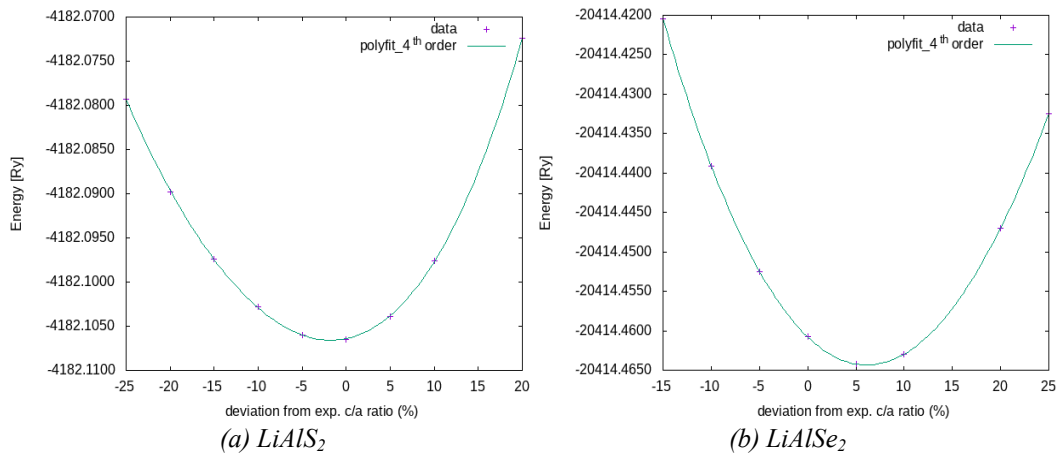


Fig. 2. Optimization curves of lattice constants as a function of total energy for  $\text{LiAlX}_2$  ( $X=\text{S}$  and  $\text{Se}$ ) ternary chalcopyrites.

### 3.2. Electronic properties

#### 3.2.1. Bandgap, Band Structure Curve and Density of States

By doing the computation of band structure and total density of states we can figure out the electronic properties of the chosen ternary semiconductors. For this calculation we have used the PBE-GGA exchange correlation functional potential, Figure 3 represents the calculated band structure curves of  $\text{LiAlX}_2$  ( $X=\text{S}$  and  $\text{Se}$ ). From the calculation of band structure curve, it is clear that both ternary semiconductor compounds are direct band gap semiconductors because the top of valence band and the bottom of conduction band located at the similar ( $\Gamma$ - $\Gamma$ ) proportion edge. Table 3 contained the calculated along with the experimentally extracted band gaps of  $\text{LiAlS}_2$  and  $\text{LiAlSe}_2$  ternary semiconductor compounds. For comparison of results and for getting the accurate value of band gaps we have been used LDA, PBE-GGA, PBEsol-GGA and WC-GGA exchange correlation potentials and here we have found that the PBE-GGA potential gives the close values of band gaps with experimentally calculated band gaps. Also, we notice that the band gap decreasing from S to Se respectively which satisfies the theory i.e., higher atomic number compound having lesser value of band gaps. For doing the deep study of electronic properties of the chosen compounds we have calculated the DoS (Density of States) which is depicted in Figure

4 and from Figure 3 and 4 we have concluded that the computed band structure curve and the calculated DoS of these compounds are iso-electronic.. The calculation of DoS has been done by using the PBE-GGA approximation. In the DoS plots of chosen compounds the Fermi level is settled at 0 eV, left part towards Fermi level is the valence band region which is divided in two sections, the major contribution takes place in VB region as compare to the CB region of the compounds. In VB region from -6 eV to 0 eV the hybridization of s-state of Al-atom and p-state of S-atom and Se-atom i.e., sp-hybridization in VB takes place and, in the CB, region ranges from 2 eV to 6 eV sp-hybridization takes place due to the s-state of Al-atom and small contribution of p-state of S and Se-atoms, this contribution is mainly due to the Al, S and Se-atoms also there is negligible contribution takes place of d-state of Li-atom.

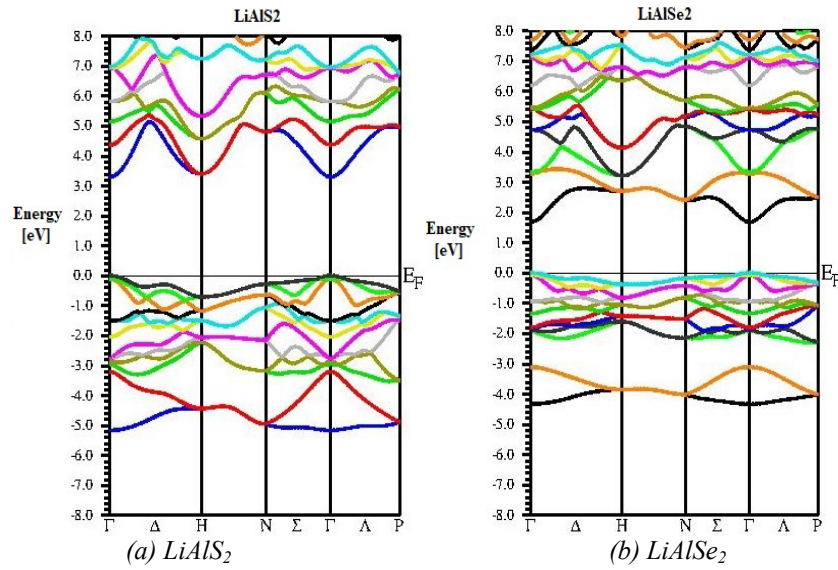


Fig. 3. Obtained bandstructure curves of  $\text{LiAlX}_2$  ( $X=\text{S}$  and  $\text{Se}$ ) ternary chalcopyrites.

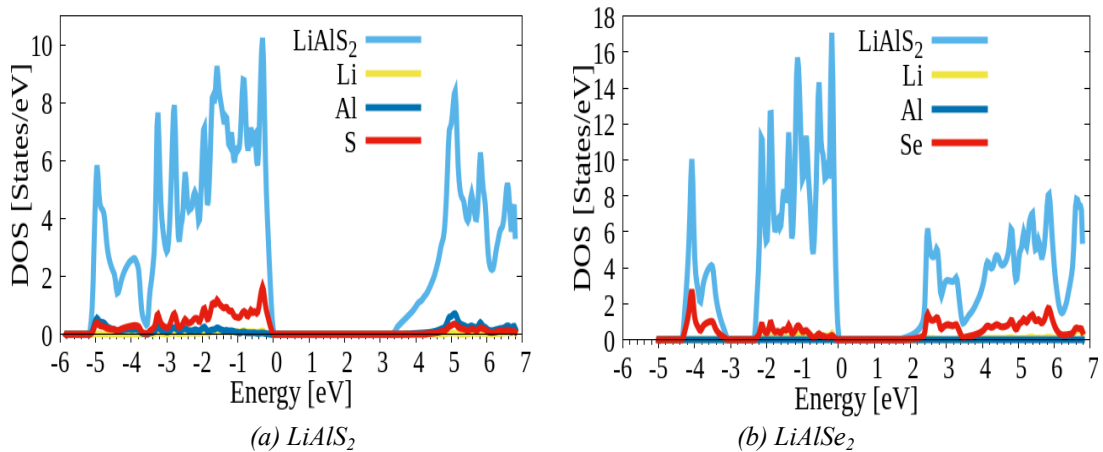


Fig. 4. Obtained Density of states of  $\text{LiAlX}_2$  ( $X=\text{S}$  and  $\text{Se}$ ) ternary chalcopyrites.

Table 3. The Calculated along with experimental Band-gaps of  $\text{LiAlX}_2$  ( $X=\text{S}$  and  $\text{Se}$ ) ternary chalcopyrites.

Compounds	Band-Gap in Electron Volt [eV]				Experimental
	LDA	WC	PBE	PBE-sol	
$\text{LiAlS}_2$	3.091	3.140	3.315	3.141	3.130 <sup>(a)</sup>
$\text{LiAlSe}_2$	1.531	1.623	1.704	1.633	1.740 <sup>(a)</sup>

<sup>(a)</sup>Ref [28].

### 3.3. Thermoelectric properties

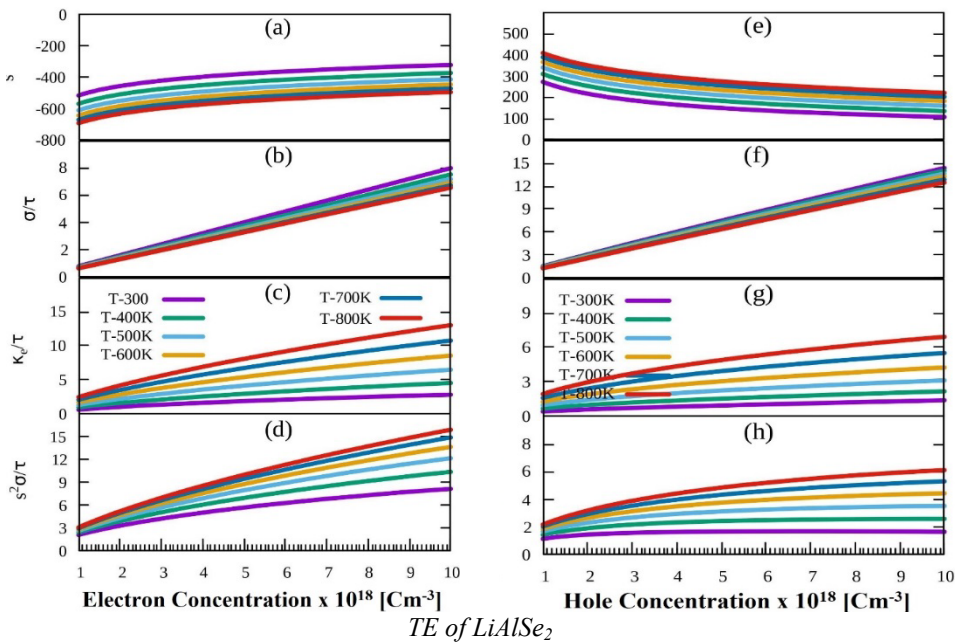
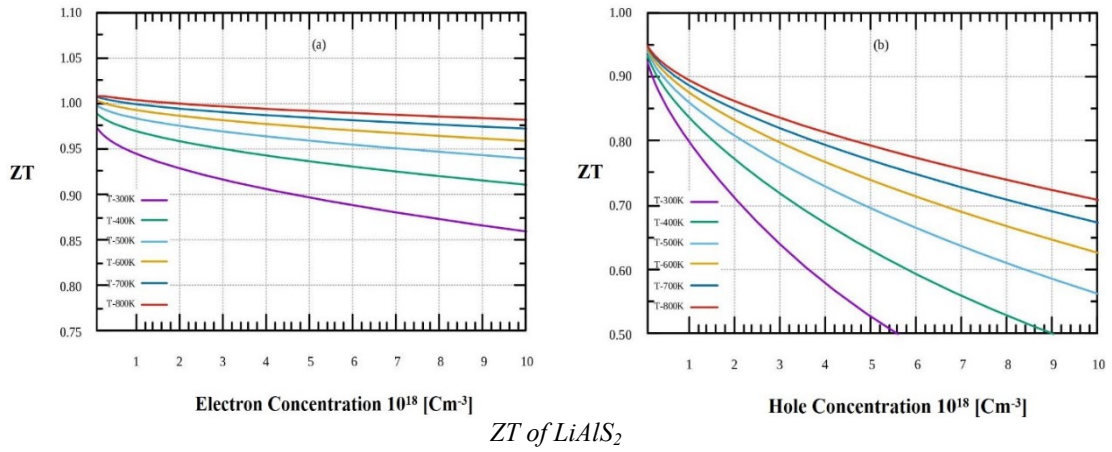
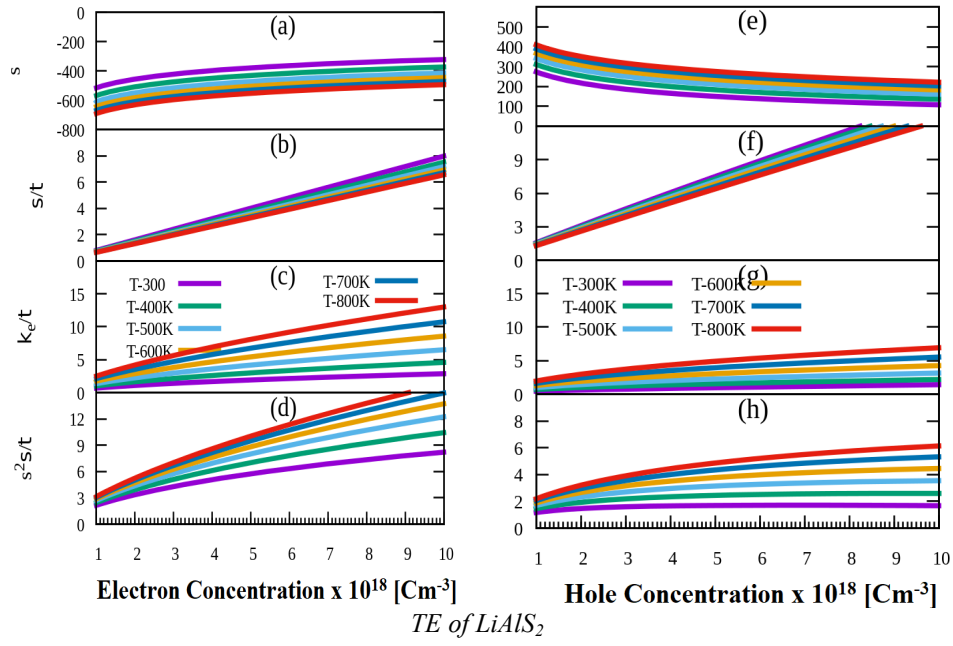
The thermoelectric properties of  $\text{LiAlS}_2$  and  $\text{LiAlSe}_2$  semiconductors have been calculated using with Boltzmann theory [29] also these parameters are depending upon the electronic structure of the compounds. When the doping in thermoelectric materials is not too high, we have used this theory for theoretical calculations of thermoelectric parameters [30]. From the electronic properties, it is ensured that these compounds  $\text{LiAlS}_2$  and  $\text{LiAlSe}_2$  possess semiconducting nature and possess direct band gap 3.315 eV and 1.704 eV, which is closest to experimental results i.e., 3.130 eV and 1.740 eV and showing good results. A. Khan *et al.* (2018) [28] have reported that why we have choose these compounds for the calculations of thermoelectric parameters. By calculating the figure of merit  $ZT = S^2\sigma T/\kappa_{total}$  we have determined the maximum efficiency of a thermoelectric compound, here ' $S^2\sigma$ ' is called the power factor, ' $S$ ' stands for Seebeck coefficient, ' $\sigma$ ' stands for electrical conductivity, ' $T$ ' stands for the absolute temperature and the addition of electrons and lattice response to the thermal conductivity is denoted by  $\kappa_{total} = \kappa_e + \kappa_l$  respectively. Here ' $\kappa_e$ ' denotes the electronic thermal conductivity and ' $\kappa_l$ ' denotes the lattice thermal conductivity correspondingly. The electrical conductivity is defined as  $\sigma = ne\mu$ , here ' $n$ ' stands for the concentration of charge carriers, ' $\mu$ ' stands for the mobility and ' $e$ ' stands for the charge of electrons. The mobility for holes is defined as  $\mu_h = \frac{e\tau_h}{m_h^*}$ , here  $\tau_h$  stands for the relaxation time of holes and  $m_h^*$  stands for the mass of holes and the mobility for electrons is defined as  $\mu_e = \frac{e\tau_e}{m_e^*}$ , here  $\tau_e$  stands for the relaxation time of electrons and  $m_e^*$  stands for the mass of electron respectively. Therefore, if the effective mass of the charge carriers is higher than the mobility as well as the electrical conductivity of the charge carriers will be smaller. Basically, the heavy charge transporters are beneficial for refining the Seebeck coefficient. We have calculated the Seebeck coefficient ' $S$ ' eccentrically at all variable constraint by using the constant relaxation time approach but we have to calculate the ' $\kappa_e$ ' and the ' $\sigma$ ' for the relaxation time ( $\tau$ ); consequently, we have been calculated the power factor in terms of relaxation time ( $S^2\sigma/\tau$ ) in the place of determining the actual power factor  $S^2\sigma$ . We are interested to figure out the Seebeck coefficient along with the band structure curve, because it defines the dominancy of the charge carriers of materials. The positive and the negative values of this coefficient show the p and n-type doping in the specimen. The variation of Seebeck coefficient as a function of charge carrier and temperatures, for  $\text{LiAlX}_2$  ( $X=\text{S}$  and  $\text{Se}$ ) as shown in the Figure 5. In this figure, consists of two regions, one is for electrons concentration i.e., n-type region and other one is for hole concentration i.e., p-type region. It is noticed that the Seebeck coefficient is rising slowly when we rising the temperature. The calculated electrical conductivity ( $\sigma/\tau$ ) has shown in Figure 5, it is observed that at different temperatures, the  $\sigma/\tau$  displays approximately slight changes. The slight change in electrical conductivity of the mentioned compounds occurred due to the variability of their electronic band gaps. We have calculated the electronic thermal conductivity ( $\kappa_e/\tau$ ) at different temperatures 300 K, 400 K, 500 K, 600K, 700 K and 800K and dependent with carrier concentration, which is shown in Figure 5. As we know the electronic thermal conductivity should be low for getting the max-to-max efficiency. From the Figure 5, we have seen that it is higher at 800 K and low at the lower temperature 300K, Also, it is observed that in the areas where the mentioned compounds acquire the lowest value of thermal conductivity are nearly the same regions in which the ' $S$ ' of mentioned compounds acquires larger values. For different carrier

concentration, and at a fixed temperature, the thermal conductivity is analogous to electrical conductivity. Moreover, we have calculated the power factor (P. F.) in the terms of relaxation time ( $S^2\sigma/\tau$ ), shown in Figure 5. We have observed that the P.F. acquire the lowest value when carrier concentration goes closer to the middle of the electronic band gaps and at the similar point the value of 'S' goes to nearly zero also the electrical conductivity almost negligible. We have seen from the graph of P.F. at 800 K it acquires the highest value and then started decreasing with decreasing the temperature. All calculated thermoelectric parameters have been tabulated in the Table 4. We have calculated  $ZT = S^2\sigma T/\kappa_{total}$ ; the figure of merit which is based on the above calculated thermal coefficients. As we know that  $S^2\sigma$  called power factor comes in numerator of ZT. It means that it plays an important role in calculating the figure of merit of the mentioned compounds. If we want the higher value of ZT lower should be the value of  $\kappa_{total}$  and higher should be the value of P.F. The calculated ZT for these compounds are shown in the Figure 6.

*Table 4. The calculated thermoelectric parameters: Seebeck coefficient  $S$  ( $\mu V/K$ ), electrical conductivity per unit relaxation time  $\sigma/\tau$  ( $\Omega ms$ )<sup>-1</sup>, power factor per unit relaxation time  $S^2\sigma/\tau$   $W/mK^2s$  and figure of merit ( $ZT = S^2\sigma T/\kappa_{total}$ ) as a function of charge carriers of  $LiAlX_2$  ( $X=S$  and  $Se$ ) ternary chalcopyrites at different temperature (300K-800K) and carrier concentration (n-type and p-type)  $10^{18}$  to  $10^{19} cm^{-3}$ .*

Compounds		S		$\sigma/\tau$		P. F		ZT	
		300 K	800 K	300 K	800 K	300 K	800 K	300 K	800 K
LiAlS <sub>2</sub>	p-type	300	400	2	1	2	1	0.956	1.011
	n-type	-500	-700	1	0.98	2	3	0.966	1.000
LiAlSe <sub>2</sub>	p-type	300	400	1.98	1	2	1	0.971	0.998
	n-type	-500	-700	1	0.979	2	3	0.926	0.972

The calculated values of ZT in the n and p-type regions at the 300 K and 800 K of the chosen materials have given in the Table 4, it is concluded that the mentioned compounds having the value of ZT at 300 K and 800 K lies in the range of 0.966 to 1.011 in n-type region and 0.965 to 1.001 for the p-type region correspondingly. It means that the observed values of the figure of merits of the mentioned materials in n-type region are 0.966 and 1.011 and 0.988 and 0.999 are in p-type region correspondingly.



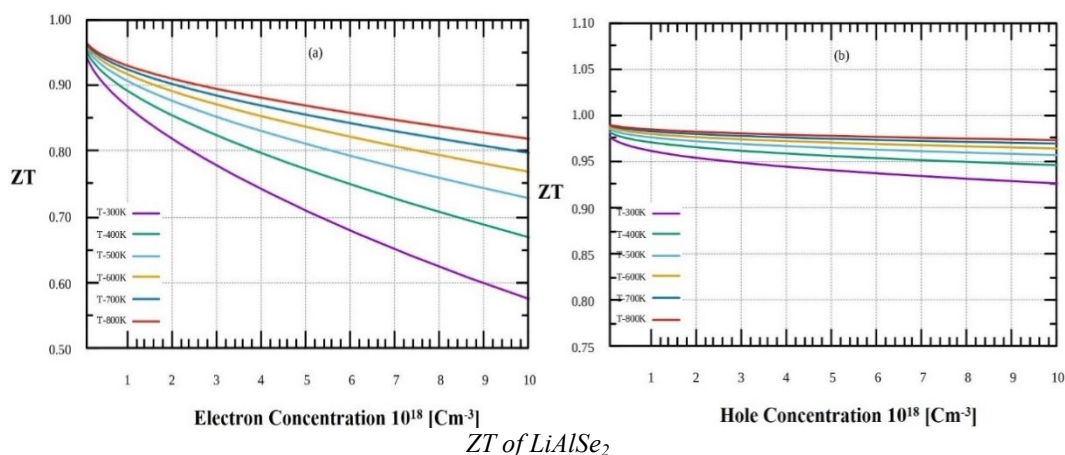


Fig. 5. The calculated Seebeck coefficient ( $S$  in  $\mu\text{V}/\text{K}$ ), Electrical conductivity per unit relaxation time  $\sigma/\tau$  ( $\Omega\text{ms}$ )<sup>-1</sup> Electronic thermal conductivity per unit relaxation time ( $\kappa_e/\tau$ ), Power Factor per unit relaxation time  $S^2\sigma/\tau$  ( $\text{W}/\text{mK}^2\text{s}$ ) and Figure of merit ( $ZT = S^2\sigma T/\kappa_{\text{total}}$ ) as a function of charge carriers at 300 K to 800 K absolute temperatures of  $\text{LiAlX}_2$  ( $X=\text{S}$  and  $\text{Se}$ ) ternary chalcopyrites. Moreover, the negligible decrement has been noticed at 800 K comparing with 300 K.

From the study of  $ZT$ , we have concluded that for the chosen compounds; its calculated value reaches to ‘unity’. Also, the investigation of this thermoelectric parameters of  $\text{LiAlX}_2$  ( $X=\text{S}$  and  $\text{Se}$ ) ensure that these semiconducting materials can turn into the promising candidate as thermoelectric substances at the room temperature and also at higher temperature too which can be the beneficial for the generation of electric power for the thermoelectric devices [31-33].

#### 4. Summary and conclusions

In this scientific research work we have reported the structural, electronic and thermoelectric properties of  $\text{LiAlX}_2$  ( $X=\text{S}$  and  $\text{Se}$ ) chalcopyrite structured semiconducting materials with the help of using wien2k simulation code based on density functional theory (DFT). The mentioned compounds possess body centred tetragonal structure and they are having direct band gap 3.13 eV for  $\text{LiAlS}_2$  and 1.74 eV for  $\text{LiAlSe}_2$ . These compounds are having the value (1.011 in n-type region and 1.001 for the p-type region) of  $ZT$  at 800 K. So, these investigated parameters prove that these compounds may be selected as the potential materials for using in thermoelectric power generators as a resource of green and renewable energy. We are expecting that this research work will prove beneficial for upcoming scientific researches in the connected field of research.

#### References

- [1] J. Kumari, S. Tomar, Sukhendra, B. L. Choudhary, U. Rani, and A. S. Verma, East European Journal of Physics, 3, 62-69 (2021); <https://doi.org/10.26565/2312-4334-2021-3-09>
- [2] W. Sukkabot, Philosophical Magazine. 101, 2157 (2021); <https://doi.org/10.1080/14786435.2021.1954257>
- [3] P. Janicek, V. Kucek, J. Kasparova, T. Plechacek, E. Cernoskova, L. Benes, M. Munzar, and C. Drasar, J. Elec. Mater. 48, 2112 (2019); <https://doi.org/10.1007/s11664-019-06993-2>
- [4] J. J. Arias, D. S. Daz, and D. A. Rasero Causila, Eur. Phys. J. B. 92,112 (2019).
- [5] K. Liu, M. Ji, H. Li, and C. Xu, Integr. Ferroelectr. 197, 33 (2019); <https://doi.org/10.1080/10584587.2019.1592076>
- [6] M. Hamid, S. A. Fadaam, L. A. Mohammed, and B. H. Hussein, Eurasian Chem. Technol. J.

- 21, 183 (2019); <https://doi.org/10.18321/ectj859>
- [7] A. S. Kshirsagar, P.V. More, P.K. Khanna, RSC Adv. 6, 86137 (2016); <https://doi.org/10.1039/C6RA16933C>
- [8] J.Y. Choi, S. J. Lee, W. S. Seo, H. Song, Cryst. Eng. Comm. 18, 6069 (2016); <https://doi.org/10.1039/C6CE00950F>
- [9] M. Mobarak, H.T. Shaban, Mater. Chem. Phys.147, 439 (2014); <https://doi.org/10.1016/j.matchemphys.2014.05.012>
- [10] V. Dubrovskii, A. Koryakin, N. Sibirev, Mater. Des.132, 400 (2017); <https://doi.org/10.1016/j.matdes.2017.07.012>
- [11] D. R. Pernik, M. Gutierrez, C. Thomas, V.R. Voggu, Y.X. Yu, J. van Embden, A.J. Topping, J. J. Jasieniak, D.A. Vanden Bout, R. Lewandowski, B.A. Korgel, ACS Energy Lett. 1 (5),1021 (2016); <https://doi.org/10.1021/acseenergylett.6b00470>
- [12] J. Li, Q. Tan, and J. F. Li, J. Alloys. Compd. 551, 143 (2013); <https://doi.org/10.1016/j.jallcom.2012.09.067>
- [13] S. Ghosh, T. Avellini, A. Petrelli, I. Kriegel, R. Gaspari, G. Almeida, G. Bertoni, A. Cavalli, F. Scotognella, T. Pellegrino, and L. Manna, Chem. Mater. 28, 4848 (2016); <https://doi.org/10.1021/acs.chemmater.6b02192>
- [14] A. Nomura, S. Choi, M. Ishimaru, A. Kosuga, T. Chasapis, S. Ohno, G. J. Snyder, Y. Ohishi, H. Muta, S. Yamanaka, and K. Kurosaki, ACS Appl. Mater. Interfaces. 10, 43682 (2018); <https://doi.org/10.1021/acsami.8b16717>
- [15] S. Twaha, J. Zhu, Y. Yan, B. Li, Ren. Sus. Ene. Rev. 65, 698 (2016); <https://doi.org/10.1016/j.rser.2016.07.034>
- [16] T. Ghellab, H. Baaziz, Z. Charifi, K. Bouferrache, S. Ugur, G. Ugur and H. Unver, International J. Modern Physics B. 33, 1950234 (2019); <https://doi.org/10.1142/S0217979219502345>
- [17] W. Khan, A.H. Reshak, Computational Materials Science. 89, 52 (2014); <https://doi.org/10.1016/j.commatsci.2014.03.028>
- [18] V. V. Atuchin, F. Liang, S. Grazhdannikov, L. I. Isaenko, P. G. Krinitsin, M. S. Molokeyev, I. P. Prosvirin, X. Jiange and Z. Lin, RSC Adv. 8, 9946 (2018); <https://doi.org/10.1039/C8RA01079J>
- [19] A. Kurus, A. Yelisseyev, S. Lobanov, P. Plyusnin, M. Molokeyev, L. Solovyev, D. Samoshkin, S. Stankus, S. Melnikova and L. Isaenko, RSC Adv. 11, 39177 (2021); <https://doi.org/10.1039/D1RA05698K>
- [20] P. Blaha, K. Schwarz, G. K. Madsen, D. Kvasnicka, J. Luitz, R. Laskowski, F. Tran, L. D. Marks, "Wien2k: An augmented plane wave plus local orbitals program for calculating crystal properties (revised edition)", Vienna University of Technology, Austria. (2018).
- [21] E. Wimmer, H. Krakauer, M. Weinert, & A. J. Freeman, Phys. Rev. Letter. 24, 864 (1981); <https://doi.org/10.1103/PhysRevB.24.864>
- [22] W. Kohn and L. J. Sham, Physical Review. 140, A1133 (1965); <https://doi.org/10.1103/PhysRev.140.A1133>
- [23] J.P. Perdew, K. Burke, M. Ernzerhof, Phys. Rev. Letter.77, 3865 (1996); <https://doi.org/10.1103/PhysRevLett.77.3865>
- [24] J. P. Perdew, A. Ruzsinszky, G. I. Csonka, O. A. Vydrov, G. E. Scuseria, L. A. Constantin, K. Burke, Physical Review Letters. 100, 136406 (2008); <https://doi.org/10.1103/PhysRevLett.100.136406>
- [25] Z. Wu, & R. E. Cohen, Phys. Rev. B. 73, 235116 (2006).
- [26] G. K. H. Madsen and D. J. Singh, Computer Physics Communications. 175, 67 (2006); <https://doi.org/10.1016/j.cpc.2006.03.007>
- [27] F. D. Murnaghan, Proc. Natl. Acad. Sci. USA 30, 244 (1947); <https://doi.org/10.1073/pnas.30.9.244>
- [28] A. Khan, M. Sajjad, G. Murtaza and A. Laref, Zeitschrift für Naturforschung A, 73 645 (2018); <https://doi.org/10.1515/zna-2018-0070>

- [29] T. J. Scheidemantel, C. Ambrosch-Draxl, T. Thonhauser, J.V. Badding, J.O. Sofo, Phys. Rev. B. 68, 125210 (2003); <https://doi.org/10.1103/PhysRevB.68.125210>
- [30] L. Chaput, P. Pecher, J. Tobola, H. Scherrer, Phys. Rev. B. 72, 085126 (2005); <https://doi.org/10.1103/PhysRevB.72.085126>
- [31] S. Pachori, R. Agarwal, B. Prakash, S. Kumari, and A. S. Verma, Energy Technology 10 2100709 (2022); <https://doi.org/10.1002/ente.202100709>
- [32] S. Pachori, R. Agrawal, A. Shukla, and A. S. Verma, Materials Chemistry and Physics, 287 126149 (2022); <https://doi.org/10.1016/j.matchemphys.2022.126149>
- [33] S. Pachori, R. Agarwal, A. Shukla, U. Rani, and A. S Verma, International J. Quantum Chemistry 121, e26671 (2021); <https://doi.org/10.1002/qua.26671>